Published in final edited form as:
Cell. 2014 January 30; 156(3): 413–427. doi:10.1016/j.cell.2013.12.023.

DNA Damage Triggers Golgi Dispersal via DNA-PK and GOLPH3

Suzette E. Farber-Katz[1], **Holly C. Dippold**[1], **Matthew D. Buschman**[1], **Marshall C. Peterman**[1], **Mengke Xing**[1], **Christopher J. Noakes**[1], **John Tat**[1], **Michelle M. Ng**[1], **Juliati Rahajeng**[1], **David M. Cowan**[1], **Greg J. Fuchs**[2], **Huilin Zhou**[2], and **Seth J. Field**[1,*]

[1]Division of Endocrinology and Metabolism Department of Medicine University of California San Diego La Jolla CA 92093-0707 USA

[2]Ludwig Institute for Cancer Research University of California San Diego La Jolla CA 92093-0653 USA

SUMMARY

The response to DNA damage, which regulates nuclear processes such as DNA repair, transcription, and cell cycle, has been studied thoroughly. However, the cytoplasmic response to DNA damage is poorly understood. Here, we demonstrate that DNA damage triggers dramatic reorganization of the Golgi, resulting in its dispersal throughout the cytoplasm. We further show that DNA-damage-induced Golgi dispersal requires GOLPH3/MYO18A/F-actin and the DNA damage protein kinase, DNA-PK. In response to DNA damage, DNA-PK phosphorylates GOLPH3, resulting in increased interaction with MYO18A, which applies a tensile force to the Golgi. Interference with the Golgi DNA damage response by depletion of DNA-PK, GOLPH3, or MYO18A reduces survival after DNA damage, whereas over-expression of GOLPH3, as is observed frequently in human cancers, confers resistance to killing by DNA-damaging agents. Identification of the DNA-damage-induced Golgi response reveals an unexpected pathway through DNA-PK, GOLPH3, and MYO18A that regulates cell survival following DNA damage.

INTRODUCTION

DNA damage is well known to trigger the activation of DNA repair, cell-cycle arrest, and transcriptional changes. These nuclear effects of DNA damage have been studied extensively (Ciccia and Elledge, 2010; Lord and Ashworth, 2012; Morandell and Yaffe, 2012). By contrast, little is known regarding the regulation of cytoplasmic organelles, such as the Golgi, in response to DNA damage. Our studies, described here, of the regulation of the Golgi protein GOLPH3 (also known as GMx33, GPP34, and yeast Vps74p; Bell et al., 2001; Schmitz et al., 2008; Snyder et al., 2006; Tu et al., 2008; Wu et al., 2000) identify a direct signaling pathway initiated by DNA damage that leads to dramatic reorganization of the Golgi.

*Correspondence: sjfield@ucsd.edu.

SUPPLEMENTAL INFORMATION

Supplemental Information includes Extended Experimental Procedures, seven figures, and four movies and can be found with this article online at http://dx.doi.org/10.1016/j.cell.2013.12.023.

We previously demonstrated that GOLPH3 is an effector of PtdIns(4)P that links *trans*-Golgi membranes to the unconventional myosin MYO18A and to the actin cytoskeleton (Dippold et al., 2009). We found that the PtdIns(4)P/GOLPH3/MYO18A/ F-actin pathway applies a tensile force to the Golgi, stretching the Golgi ribbon around the nucleus and promoting vesicle exit from the Golgi (Bishé et al., 2012; Dippold et al., 2009; Ng et al., 2013). Unexpectedly, unbiased screening identified GOLPH3 as an oncogene that is amplified in human cancers (Scott et al., 2009), and GOLPH3 overexpression occurs frequently and has negative prognostic significance in several cancers (Hu et al., 2013; Hua et al., 2012; Kunigou et al., 2011; Li et al., 2012, 2011; Wang et al., 2012; Zeng et al., 2012; Zhou et al., 2012).

Here, we demonstrate that in mammalian cells, DNA damage triggers the Golgi to fragment and disperse throughout the cytoplasm. This response requires the direct phosphorylation of GOLPH3 on T143/T148 by DNA-PK, resulting in enhanced interaction between GOLPH3 and MYO18A. Thus, we show that common cancer therapeutic agents, by triggering DNA damage, activate GOLPH3, a proven oncogene. We find that the DNA-PK/GOLPH3/MYO18A pathway is required for normal survival following DNA damage. Furthermore, overexpression of GOLPH3 confers resistance to killing by DNA-damaging agents. Thus, we identify a novel pathway that is activated by DNA damage and signals directly to the Golgi, with important consequences for the cellular response to chemotherapeutic agents.

RESULTS

DNA Damage Causes Dispersal of the Golgi

GOLPH3 has been shown to be a phosphoprotein (Wu et al., 2000), although the sites of phosphorylation were previously unidentified. Using large-scale immunoprecipitation (IP) of GOLPH3 followed by mass spectrometry, we observe that T143 and T148 are phosphorylated together on GOLPH3 (Figure 1A). We note that T143 is followed by a glutamine at the +1 position, thereby comprising a “TQ” motif that is highly conserved among vertebrate GOLPH3 orthologs. TQ/SQ is the preferred substrate motif for phosphorylation by the DNA-damage-activated protein kinases ATM, ATR, and DNA-PK (Kim et al., 1999; O'Neill et al., 2000). Interestingly, TVQ at T148 also conforms to an alternate preferred substrate motif for ATM and DNA-PK (Anderson, 1993; O'Neill et al., 2000; Obenauer et al., 2003).

Because little was known regarding the effects of DNA damage on the Golgi, and because of GOLPH3's role in maintaining Golgi shape, we examined whether DNA damage affects Golgi morphology. We treated human embryonic kidney 293 (HEK293) cells with camptothecin (CPT), doxorubicin (DOXO), or ionizing radiation (IR) to induce DNA damage. Exposure to each treatment caused Golgi morphology to change dramatically from the usual perinuclear ribbon to punctate fragments dispersed throughout the cytoplasm (Figure 1B; Movies S1 and S2 available online). We quantified Golgi dispersal by measuring the Golgi area per cell, which significantly increased as doses of CPT, DOXO, and IR increased (Figures 1C and 1D). Even low doses of DNA-damaging agents that caused little or no apparent cytotoxicity caused significant Golgi dispersal.

Golgi dispersal in response to DNA damage occurred in many cell lines (HEK293, HeLa, NRK, MCF7, and MDA-MB-231), as well as in primary mouse embryonic fibroblasts, primary mouse hepatocytes, and primary human umbilical vein endothelial cells (HUVECs) (Figures 1B–1D, S1A–S1H, S3D, and S3E; data not shown). Thus, Golgi dispersal is a common feature of the DNA damage response in mammalian cells.

We further analyzed the kinetics of Golgi dispersal after DNA damage. As shown in Figure 2A and Movies S1 and S2, in HeLa cells dispersal of the Golgi was detectable within 4 hr after treatment with DNA-damaging agents and progressively increased over 24 hr. Long-time-course experiments in which HeLa cells were treated with DOXO for 24 hr, followed by drug washout, revealed that the most dramatic Golgi dispersal persisted for at least 5 days (Figure S2A). Moreover, the Golgi remained detectably dispersed at least 30 days after the initial DNA damage occurred (Figure 2B), at a time when cell proliferation has completely recovered (van Vugt and Yaffe, 2010).

Although the Golgi dispersed in response to DNA damage, it remained intact, as markers for the *cis*-Golgi (GM130), *medial*-Golgi (α-mannosidase II [ManII]), and *trans*-Golgi (p230, GOLPH3, and TGN46) all remained colocalized (Figures 3A, 4A, 5A, 6A, S1A, and S5A). We compared the Golgi localization of EYFP-FAPP1-PH, a reporter for PtdIns(4)P (Dippold et al., 2009; Godi et al., 2004), before versus after treatment with DNA-damaging agents (Figures S1I and S1J). We did not observe qualitative or quantitative changes, arguing that PtdIns(4)P levels at the Golgi are unchanged by DNA damage. The dispersed Golgi remained distinct from other punctate organelles, as shown by a lack of colocalization with markers for early endosomes or lysosomes (Figures S2B and S2C). Notably, these other organelles appeared to be unchanged by DNA damage.

DNA-Damage-Induced Golgi Dispersal Occurs Independently of Apoptosis

We next examined candidate mechanisms of DNA-damage-induced Golgi dispersal. Since changes in Golgi morphology have been reported to occur during apoptosis (Chiu et al., 2002; Jung et al., 2006; Lane et al., 2002; Mancini et al., 2000; Qian and Yang, 2009), we examined whether DNA-damage-induced Golgi dispersal occurs as a consequence of apoptosis. Although treatment with CPT caused a significant increase in the number of apoptotic cells (Figures 2C and 2D), still only a small fraction of cells became apoptotic (1.74% ± 0.08% [mean ± SEM] positive for cleaved caspase-3 (CCasp-3), coinciding with other morphological evidence of apoptosis, such as pyknotic nuclei, fragmented nuclei, or plasma membrane [PM] blebbing). The Golgi in these apoptotic cells do exhibit abnormal morphology, as expected. By contrast, the nonapoptotic cells, which constitute the majority of cells, display a uniformly dispersed Golgi. The addition of an apoptosis inhibitor, zVAD-fmk, significantly decreased the number of apoptotic cells produced in response to CPT, without impeding the dispersal of the Golgi (Figure 2D), indicating that Golgi dispersal following DNA damage occurs independently of apoptosis.

Long-time-course time-lapse imaging shows that cells with a dispersed Golgi after DNA damage remained alive and healthy, without any morphological evidence of apoptosis, during at least 17 hr of follow-up imaging (Movies S1 and S2). Likewise, days to weeks following low doses of DNA-damaging agents, at times when the cells had otherwise

completely recovered, we observed persistent changes in Golgi morphology (Figures 2B and S2A). Taken together, these results indicate that DNA-damage-induced dispersal of the Golgi occurs independently of apoptosis.

DNA-Damage-Induced Golgi Dispersal Is Unlike Microtubule Depolymerization

Depolymerization of microtubules by nocodazole is known to cause Golgi dispersal (Thyberg and Moskalewski, 1999). Therefore, we examined whether Golgi dispersal in response to DNA damage appears similar to the response to nocodazole treatment and hence might be mechanistically related. Microtubule depolymerization produces a dispersed Golgi that is closely apposed to the transitional endoplasmic reticulum (tER; Hammond and Glick, 2000). When HeLa cells were treated with nocodazole for 1 hr, we observed Golgi dispersal and its association with Sec31A, a marker of the tER (Figure S2D). By contrast, after DNA damage, the dispersed Golgi remained independent of the tER. Moreover, addition of nocodazole after CPT resulted in further Golgi reorganization, with association with the tER. Quantification of Golgi dispersal induced by nocodazole, DNA damage, or the combination of the two demonstrated an additive effect of combining the two treatments (Figure S2E). Thus, DNA-damage-induced Golgi dispersal is mechanistically distinct from the dispersal induced by nocodazole.

We also considered whether the dispersal of the Golgi after DNA damage might be a consequence of cell-cycle arrest in early mitosis, when the Golgi normally fragments (Wei and Seemann, 2009). However, consistent with published data (Hennequin et al., 1994; Hsiang et al., 1989; Maney et al., 2011), HeLa cells and HUVECs treated with CPT arrested in G1 or early S phase (Figures S2F and S2G; see also Movie S2), part of the cell cycle during which the Golgi generally remains intact. Furthermore, long-time-course experiments demonstrated persistence of Golgi dispersal even after cell proliferation had recovered (Figures 2B and S2A). We conclude that arrest in M phase is not the mechanism of DNA-damage-induced Golgi dispersal.

GOLPH3, MYO18A, and F-actin Are All Required for DNA-Damage-Induced Golgi Dispersal

Because of the important role of GOLPH3/MYO18A/F-actin in the maintenance of Golgi morphology (Dippold et al., 2009; Ng et al., 2013) and the presence of a phospho-TQ site in GOLPH3, we tested whether GOLPH3 and MYO18A are required for DNA-damage-induced dispersal of the Golgi. We depleted GOLPH3 or MYO18A approximately 90% after transient transfection of each of three different small interfering RNA (siRNA) oligos (Figures S3A and S3B). Depletion of GOLPH3 or MYO18A in HeLa cells prevented Golgi dispersal in response to DNA damage (Figures 3A–3C). Similar results were observed in HEK293 and HUVECs (Figures S3C–S3E). Depletion of GOLPH3 or MYO18A did not inhibit the overall DNA damage response, as DNA damage foci still formed in response to DNA-damaging agents in the knockdown cells (Figure S3F).

Since F-actin links to MYO18A and is also required for maintenance of normal Golgi morphology (Dippold et al., 2009; Lázaro-Diéguez et al., 2006), we determined whether F-actin is required for Golgi dispersal after DNA damage. As shown in Figures 3D, 3E, and Movie S3, depolymerization of F-actin led to rapid reversal of DNA-damage-induced Golgi

dispersal. Therefore, GOLPH3, MYO18A, and F-actin are all required for DNA-damage-induced dispersal of the Golgi.

Phosphorylation of the TQ Motif in GOLPH3 Is Required for DNA-Damage-Induced Golgi Dispersal

We next asked whether phosphorylation of GOLPH3 on the TQ site at T143 and the adjacent T148 is required for DNA-damage-induced dispersal of the Golgi. We mutated T143 and T148 in an siRNA-resistant GOLPH3 mammalian expression construct (wild-type [WT] sequence: TQ-TVQ) to create an unphosphorylatable mutant (AQ-AVQ) and two phosphomimetic mutants (EQ-EVQ and DQ-DVQ). We then depleted endogenous GOLPH3 protein by siRNA and expressed siRNA-resistant WT or mutant GOLPH3. As described previously, knockdown of GOLPH3 resulted in a compact Golgi morphology (Dippold et al., 2009; Ng et al., 2013). In the absence of DNA damage, expression of each mutant or WT protein rescued the normal extended ribbon morphology of the Golgi (Figures S4A–S4C). All mutants localized to the Golgi and all bound strongly to PtdIns(4)P (Figures S4D and S4E). Restoration of GOLPH3 protein levels with WT or either phosphomimetic mutant rescued the dispersal after DNA damage (Figures 4A and 4B). By contrast, although the unphosphorylatable mutant rescued extended Golgi morphology in the absence of DNA damage, it failed to rescue DNA-damage-induced dispersal of the Golgi. We conclude that phosphorylation of T143/T148 on GOLPH3 is necessary (although alone is not sufficient) for DNA-damage-induced Golgi dispersal.

DNA-PK Is Required for Golgi Dispersal after DNA Damage

Because phosphorylation of GOLPH3 on T143/T148 is required for DNA-damage-induced Golgi dispersal, we sought to identify the responsible kinase. The two main kinases that phosphorylate TQ or SQ motifs and are activated in response to double-stranded DNA breaks are ATM and DNA-PK (Ciccia and Elledge, 2010; O'Neill et al., 2000). We treated cells with inhibitors specific for ATM (KU55933; Hickson et al., 2004) or DNA-PK (NU7441; Tavecchio et al., 2012) and analyzed Golgi morphology after DNA damage. Treatment with KU55933 minimally prevented Golgi dispersal in response to DNA damage by CPT or IR, whereas treatment with NU7441 completely prevented DNA-damage-induced dispersal of the Golgi (Figures S5A–S5C).

We further tested a requirement for ATM using ATM-deficient A-T fibroblasts derived from a patient with ataxia telangiectasia. In parallel, we examined A-T fibroblasts that were reconstituted with ATM. In A-T cells with or without reconstitution of ATM, the Golgi dispersed similarly after DNA damage. In these cells, treatment with KU55933 had little effect, whereas NU7441 again completely prevented DNA-damage-induced dispersal of the Golgi (Figures 5A–5C). We conclude that ATM is not required for DNA-damage-induced dispersal of the Golgi.

To confirm whether DNA-PK is required for DNA-damage-induced dispersal of the Golgi, we utilized siRNA knockdown of DNA-PK. Depletion of DNA-PK by either of two specific siRNAs (Figure S6A) prevented Golgi dispersal in response to DNA damage in HeLa

(Figures 6A and 6B), HEK293 (Figure S3C), and HUVECs (Figure S3E). Therefore, DNA-PK, but not ATM, is required for DNA-damage-induced Golgi dispersal.

The DNA-PK kinase inhibitor also allowed us to test whether DNA-PK kinase activity is required Thuso maintain Golgi dispersal after DNA damage. We treated cells with DOXO to cause dispersal of the Golgi. Addition of NU7441 caused a dramatic reversal of the Golgi dispersal (Movie S4). Thus, continuous DNA-PK kinase activity is necessary to maintain Golgi dispersal following DNA damage.

We also examined whether the related protein kinases ATR and mTOR might have a role in DNA-damage-induced Golgi dispersal. Although inhibition of DNA-PK significantly reversed Golgi dispersal, inhibition of ATR with VE821 (Charrier et al., 2011) or mTOR with Torin1 (Liu et al., 2010) did not (Figure S5D). We conclude that DNA-PK, but not the related kinases ATM, ATR, and mTOR, is specifically required for DNA-damage-induced Golgi dispersal.

DNA-PK Directly Phosphorylates GOLPH3

Because the T143 and T148 phosphorylation sites in GOLPH3 conform to the preferred and alternative substrate motifs for DNA-PK, we asked whether DNA-PK directly phosphorylates GOLPH3. First, we determined whether DNA-PK is capable of directly phosphorylating GOLPH3. Using an in vitro kinase assay, we observed that purified DNA-PK could directly phosphorylate glutathione S-transferase (GST)-GOLPH3 expressed and purified from *E. coli* (Figure 6C). This phosphorylation occurred on T143 and/or T148, as the AQ-AVQ mutation largely abolished it. Furthermore, we verified that the responsible kinase in the commercially obtained DNA-PK preparation is actually DNA-PK because the phosphorylation is completely eliminated by NU7441.

We next examined whether DNA-PK is directly responsible for GOLPH3 phosphorylation in vivo. The DNA-PK preferred phosphorylation motif requires the Q at the +1 position (O'Neill et al., 2000), whereas most other kinases have different sequence requirements (Mok et al., 2010). Therefore, we tested whether the Q at the +1 position (Q144) is required for the Golgi to respond to DNA damage. First, we created a GOLPH3 mutant, TQ-AVQ, to test whether phosphorylation on T143 (but not T148) is sufficient for DNA-damage-induced dispersal of the Golgi. Indeed, in knockdown/rescue experiments, expression of the siRNA-resistant TQ-AVQ mutant of GOLPH3 rescued Golgi dispersal after DNA damage (Figures 4A and 4B). We also created a mutant in which Q144 is mutated (TA-AVQ). This abolishment of the TQ motif tests whether direct phosphorylation by a DNA-damage-activated, TQ-directed kinase is required for Golgi dispersal. In cells expressing the TA-AVQ mutant, the Golgi failed to disperse after DNA damage (Figures 4A and 4B). Finally, we created a phosphomimetic mutant (EA-AVQ) to serve as a control to test whether the Q-to-A mutation nonspecifically inactivates GOLPH3 or instead specifically impairs phosphorylation of GOLPH3 and therefore can be rescued by a phosphomimetic mutation that restores the electrostatic features of phosphorylation. In fact, the Golgi dispersed normally after DNA damage in cells expressing the EA-AVQ mutant (Figures 4A and 4B). We conclude that both T143 and Q144, which together comprise the TQ motif, are both required for Golgi dispersal in response to DNA damage. These data, together with the

requirement for DNA-PK but not other TQ-directed kinases, strongly argue that DNA-PK directly phosphorylates GOLPH3.

Occasionally, the interaction between a kinase and its substrate is sufficiently tight to allow direct observation by coimmunoprecipitation (coIP) of a complex between them (Johnson and Hunter, 2005). To test whether GOLPH3 and DNA-PK form a stable complex, we immunoprecipitated endogenous GOLPH3 from detergent lysates of HeLa cells. We used western blotting with an antibody specific to Ku80, a regulatory subunit of DNA-PK, to determine whether the endogenous DNA-PK complex was coimmunoprecipitated. As shown in Figure 6D, in control IPs using preimmune serum, we see a minimal background precipitation of Ku80. However, specific IP of GOLPH3 is accompanied by significant coIP of Ku80, but not other irrelevant proteins. This indicates a specific physical interaction between GOLPH3 and DNA-PK.

Thus, we observe that Golgi dispersal after DNA damage requires both DNA-PK (which is known to be activated by DNA damage; Neal and Meek, 2011) and the DNA-PK substrate motif within GOLPH3. Our data also demonstrate that DNA-PK can directly phosphorylate GOLPH3 on T143 in vitro, and we detect a physical interaction between GOLPH3 and DNA-PK in cells. Taken together, these results indicate that DNA-PK directly phosphorylates GOLPH3 on T143, and that this is required for Golgi dispersal in response to DNA damage.

DNA Damage Enhances the Interaction between GOLPH3 and MYO18A

Since Golgi dispersal after DNA damage mimics Golgi dispersal after overexpression of GOLPH3 (Ng et al., 2013), we infer that phosphorylation of GOLPH3 after DNA damage enhances the function of GOLPH3. Therefore, we asked whether the response to DNA damage enhances GOLPH3's known interactions with PtdIns(4)P or MYO18A. Interaction between GOLPH3 and PtdIns(4)P is responsible for localization of the protein to the *trans*-Golgi (Dippold et al., 2009; Wu et al., 2000). GOLPH3 localization to the Golgi is unchanged after DNA damage (Figures 3A, 4A, 5A, 6A, S1A, and S5A). Likewise, phosphorylation mutants of GOLPH3 do not alter binding to PtdIns(4)P in vitro (Figure S4E), and they localize to the Golgi in cells before and after DNA damage (Figures 4A and S4A). Thus, phosphorylation of GOLPH3 on T143/T148 in response to DNA damage does not affect its binding to PtdIns(4)P.

Next, we determined whether DNA damage alters the strength of the interaction between GOLPH3 and MYO18A. Indeed, X-ray crystallographic models of GOLPH3 (Dippold et al., 2009; Schmitz et al., 2008; Wood et al., 2009) indicate that T143 and T148 are on the surface of GOLPH3 and would remain available to interact with MYO18A even after GOLPH3 is bound to the Golgi membrane. We assayed coIP of endogenous MYO18A with GOLPH3 in detergent lysates from control cells or DNA-damage-treated cells. DNA damage induced by either CPT or DOXO led to enhanced interaction of GOLPH3 with MYO18A (Figures 6E and S6B).

To determine whether phosphorylation of GOLPH3 directly increases its affinity for MYO18A, we examined the interaction of purified, bacterially expressed proteins,

comparing WT GOLPH3 (TQ-TVQ) with the phosphomimetic mutants (EQEVQ and DQ-DVQ). As previously reported (Dippold et al., 2009), WT GOLPH3 (but not the GST control) was specifically pulled down with His-SUMO-MYO18A (aa 408–1,242), but not with control His-SUMO alone (Figure 6F). Interestingly, we observed that the phosphomimetic mutants had an increased affinity for MYO18A, indicating that phosphorylation of GOLPH3 alone is sufficient to increase its interaction with MYO18A. We previously showed that GOLPH3/MYO18A/F-actin applies a tensile force to the Golgi that assists in vesiculation (Dippold et al., 2009; Ng et al., 2013). Taken together with the observation that GOLPH3, MYO18A, and F-actin are all required for Golgi dispersal in response to DNA damage, we conclude that this enhanced interaction between GOLPH3 and MYO18A contributes to DNA-damage-induced Golgi dispersal.

The DNA Damage Response Results in Impaired Golgi Trafficking

The GOLPH3/MYO18A/F-actin pathway is critical for Golgi to PM trafficking (Bishé et al., 2012; Dippold et al., 2009; Ng et al., 2013). Therefore, we examined whether changes in Golgi trafficking occur following DNA damage. Temperature-sensitive, GFP-tagged ts045-VSVG-GFP synchronously traffics from the ER through the Golgi to the PM upon a shift from a restrictive (4°C) to a permissive temperature (32°C) (Presley et al., 1997). In control cells, after the shift to 32°C, we observed trafficking from the ER through the Golgi to the PM (Figures 6G and S6C). However, after 18 hr of CPT treatment, ts045-VSVG-GFP instead accumulated at the Golgi without progressing to the PM. We conclude that DNA-damage-induced Golgi dispersal results in impaired Golgi to PM trafficking.

GOLPH3 and MYO18A Are Required for Normal Survival after DNA Damage

GOLPH3 is an oncogene that is known to modulate growth factor signaling through the mTOR pathway (Scott et al., 2009), which is known to deliver survival signals (Laplante and Sabatini, 2009; Myers and Cantley, 2010). To determine whether the DNA-PK/GOLPH3/MYO18A pathway is functionally important following DNA damage, we examined whether interference with the pathway affects survival following DNA damage. First, we examined the influence of the pathway on DNA-damage-induced apoptotic cell death. As expected, treatment of HeLa cells with DOXO caused significant apoptosis, as detected by western blot for CCasp-3 (Figure 7A). Depletion of either GOLPH3 or MYO18A by siRNA led to dramatic enhancement of CCasp-3 production after DNA damage, indicating that GOLPH3 and MYO18A participate in a pathway that protects cells from apoptosis following DNA damage. Likewise, HUVEC survival after treatment with CPT was significantly impaired by knockdown of GOLPH3 or DNA-PK (Figure S7A).

Next, we asked whether GOLPH3 or MYO18A contribute to the ability of cells to survive and proliferate following DNA damage. We used siRNA to transiently knock down GOLPH3, MYO18A, or DNA-PK, and measured clonogenic survival after 24 hr of exposure to increasing doses of DOXO. We compared the number of colonies that arose from knockdown cells with the number of colonies derived from control cells. Similar to what was observed in previous studies (Blunt et al., 1995; Peng et al., 2002), depletion of DNA-PK decreased survival after DNA damage (Figure 7B). Furthermore, transient knockdown of GOLPH3 or MYO18A at the time of DNA damage reduced survival by an

order of magnitude. Therefore, all of the components of the DNA-PK/GOLPH3/MYO18A pathway are required for normal cell survival following DNA damage.

GOLPH3 Overexpression Confers Resistance to DNA-Damaging Agents

Because normal levels of GOLPH3 protect cells from DNA-damaging agents, we wondered whether elevated levels of GOLPH3, as found frequently in human cancers, might render cells refractory to killing by DNA-damaging agents. Thus, we engineered HeLa cells to allow for doxycycline-inducible over-expression of GOLPH3 with GFP. When treated with limiting concentrations of doxycycline, ~20% of these cells coex-pressed GOLPH3 and GFP (Figure S7B; data not shown).Compared with DMSO treatment (vehicle control), brief CPT treatment for 24 hr resulted in 31% enrichment of GFP-positive/GOLPH3-overexpressing cells (Figure 7C). This enrichment is a consequence of expression of GOLPH3, as expression of GFP alone results in no enrichment. To test whether the ability of GOLPH3 to confer a survival advantage following DNA damage depends on its function at the Golgi, we examined the effect of doxycycline-induced overexpression of GOLPH3-R90L, a point mutant that is unable to bind PtdIns(4)P and thus unable to localize to the Golgi (Dippold et al., 2009). As shown in Figure 7C, cells overexpressing GOLPH3-R90L are not significantly enriched following DNA damage.

To test the role of phosphorylation of GOLPH3 in conferring a survival advantage, we compared cells that were transiently transfected with IRES-GFP constructs to express WT GOLPH3 (TQ-TVQ), unphosphorylatable GOLPH3 (AQ-AVQ), or phosphomimetic GOLPH3 (DQ-DVQ). As shown in Figure 7D, cells coexpressing WT GOLPH3 and GFP have a survival advantage over nonexpressing cells when treated with CPT. By comparison, the unphosphorylatable mutant of GOLPH3 does not confer a survival advantage, although the phosphomimetic mutant does. Thus, overexpression of GOLPH3 confers a survival advantage after DNA damage, protecting cells from killing by CPT. This function of GOLPH3 depends on binding to PtdIns(4)P, and therefore its ability to function at the Golgi, and on GOLPH3 phosphorylation on the DNA-PK site.

We next examined whether transient overexpression of GOLPH3 during DNA damage results in enhanced long-term cell survival, as measured by a clonogenic survival assay. Doxycycline was applied to the inducible cell lines for 4 days and then withdrawn to transiently raise the level of GOLPH3 (or GOLPH3-R90L or GFP alone). On day 2, replicates were replated at low density and treated with various concentrations of DOXO for 24 hr to assess clonogenic survival after 2 weeks. As shown in Figure 7E, transient overexpression of GOLPH3 (Figure S7C) at the time of a single round of DOXO treatment increased clonogenic survival by as much as 4.3-fold in a doxycycline-dose-dependent manner. By contrast, doxycycline-induced overexpression of GOLPH3-R90L or GFP alone had no signifi-cant effect on clonogenic survival after DOXO treatment (Figures S7D and S7E). Therefore, overexpression of GOLPH3 enhances the ability of cells to survive DNA damage, and this ability depends on GOLPH3's interaction with PtdIns(4)P and thus its localization to the Golgi. Taken together with the requirement for GOLPH3 in the Golgi response to DNA damage and its direct phosphorylation by DNA-PK, our results

demonstrate that DNA damage signals directly to the Golgi via GOLPH3, a pathway that we conclude is an important feature of the DNA damage response.

DISCUSSION

A Novel Response to DNA Damage

Understanding the cellular response to DNA damage is crucial for discerning the mechanisms by which many chemotherapeutic agents kill cancer cells and the mechanisms of escape from killing. Here, we demonstrate a previously poorly appreciated feature of the DNA damage response, namely, a dramatic reorganization of the Golgi. We observe that DNA damage triggered by drugs or ionizing radiation causes the Golgi to fragment and become dispersed throughout the cytoplasm. Nevertheless, *cis*-, *medial*-, and *trans*-Golgi compartments remain colocalized. Dispersal of the Golgi is observed in many cell lines as well as in primary cells, indicating that it is a ubiquitous feature of the DNA damage response in mammalian cells. The response occurs quickly and is detectable within 4 hr after exposure to DNA-damaging agents, yet it also persists for weeks after transient exposure to DNA-damaging agents. This persistence could be due to the stability of a small number of DNA breaks that continue to activate the pathway (van Vugt and Yaffe, 2010) or it may indicate the existence of a positive feedback loop that maintains the Golgi dispersal once it is initiated.

DNA-Damage-Induced Golgi Dispersal Occurs Independently of Apoptosis

The effect of DNA damage on the Golgi has been largely neglected in the literature, with a few prior hints of an effect generally being ascribed to a consequence of DNA-damage-induced apoptosis (Chiu et al., 2002; Jung et al., 2006; Lane et al., 2002; Mancini et al., 2000; Qian and Yang, 2009). The induction of Golgi dispersal by even minimally toxic doses of DNA-damaging agents, the continued apparent health of cells observed by time-lapse microscopy, and the persistence of the Golgi dispersal for weeks all demonstrate that the Golgi response is unrelated to apoptosis. Furthermore, inhibition of apoptosis does not impair DNA-damage-induced Golgi dispersal. Perhaps most significantly, we identify a direct signaling pathway from DNA-PK, a DNA-damage-activated kinase, to the Golgi protein GOLPH3, demonstrating that no intermediate steps are required at all. Finally, we find that rather than being a by-product of cell death, the pathway that is responsible for Golgi dispersal after DNA damage functions to enable cell survival after DNA damage.

DNA Damage Signals to the Golgi to Enhance Survival

The alteration in Golgi morphology after DNA damage leads ultimately to impairment of trafficking from the Golgi to the PM. However, the DNA damage response could conceivably involve initially an increase in delivery of cargoes to the PM, analogous to the effect proposed for the consequence of loss of GOLPH3L, the endogenous inhibitor of GOLPH3 that is expressed in highly secretory cells (Ng et al., 2013). In any case, we suspect that there exist one or more cargoes that depend on appropriate trafficking in order to influence cell death or survival, and that altered trafficking of these cargoes following DNA damage results in enhanced cell survival. The observation that the GOLPH3 TQ site

and DNA-PK are both restricted to higher multicellular organisms may indicate a role in balancing cell survival with organismal survival.

Implications for Cancer Prognostics and Therapeutics

Previous studies have noted that a high proportion of human cancers harbor amplification and overexpression of GOLPH3 (Hu et al., 2013; Hua et al., 2012; Kunigou et al., 2011; Li et al., 2012, 2011; Scott et al., 2009; Wang et al., 2012; Zeng et al., 2012; Zhou et al., 2012). These studies reported that overexpression of GOLPH3 correlates with a poor prognosis for several cancers, a finding that generally suggests that the cancers progress despite treatment with standard chemotherapeutics. Strikingly, we find that overexpression of GOLPH3 confers resistance to killing by DNA-damaging agents. Since DNA-damaging agents remain the mainstay of many cancer treatment regimens (Azzoli et al., 2011; Swain, 2011), this raises the possibility that GOLPH3 may be a clinically relevant marker of responsiveness to chemotherapy. Conversely, we find that interference with the GOLPH3/MYO18A pathway significantly impairs cell survival after DNA damage, suggesting that small-molecule inhibitors of the pathway may have therapeutic utility. In any case, the Golgi response to DNA damage represents a newly appreciated, fundamental aspect of cell biology that advances our understanding of the cellular response to DNA damage and reveals a direct path to the Golgi via DNA-PK and GOLPH3.

EXPERIMENTAL PROCEDURES

Kinase Assay

Kinase reactions were performed according to the DNA-PK supplier (Promega) with 1 μCi [γ-^{32}P]-ATP (Perkin Elmer). Reactions were incubated at 30°C for 30 min, stopped by the addition of boiling SDS sample buffer, run on SDS-PAGE, and visualized with a PhosphorImager (Molecular Dynamics).

Clonogenic Survival

HeLa cells were treated as described in the figure legends, replated as a dilution series, and then treated with the indicated concentrations of DOXO for 24 hr. Colonies were counted 10–14 days later.

Fluorescence Microscopy

Fluorescence microscopy was performed with an Olympus IX81-ZDC spinning-disk confocal microscope and analyzed using Slidebook and ImageJ software.

Measurement of Golgi Area

Immunofluorescent images of cells stained with a Golgi marker were measured either by manual demarcation of the Golgi with a limiting polygon and calculation of its area using ImageJ or by automated identification of the Golgi and calculation of the area of the smallest encircling ellipse as performed by CellProfiler (Carpenter et al., 2006). Both methods produced similar results.

IPs and Pull-Downs

IPs and pull-downs were performed as described previously (Dippold et al., 2009). For IP, cells were lysed in buffer containing 10 mM CHAPS. Lysates were precleared and incubated with anti-GOLPH3 or preimmune serum, bound to Protein A Sepharose (GE Healthcare), washed extensively, and eluted by boiling in SDS sample buffer. Briefly, for the pull-downs, 6xHis-SUMO and 6xHis-SUMO-tagged MYO18A motor domain (aa 408-1242) expressed in *E. coli* were bound to Ni-NTA-agarose beads (QIAGEN) and washed. A 1:1 mixture of purified GST and GOLPH3 (WT or mutant) was added to the protein-bound beads at a 1:4 molar ratio of GST/GOLPH3:6xHis-SUMO or 6xHis-SUMO-MYO18A motor domain and rotated 2 hr at 4°C in 10 mM Na_2- HPO_4, 150 mM NaCl, 20 mM imidazole, and 10 mM CHAPS (pH 7.4), followed by washing and elution in boiling SDS sample buffer for western blotting.

Mass Spectrometry

Bands were excised from polyacrylamide stained with SafeStain SimplyBlue (Invitrogen), subjected to in-gel digestion, and analyzed as described previously (Zhou et al., 2004).

Lipid Blots

Lipid blots were performed as described previously (Dippold et al., 2009). Positive controls were tested in parallel.

For further details regarding the methods and materials used in this work, see the Extended Experimental Procedures.

Supplementary Material

Refer to Web version on PubMed Central for supplementary material.

Acknowledgments

We thank Susan Ferro-Novick, M. Geoff Rosenfeld, Marilyn G. Farquhar, Jean Wang, Alexandra Newton, and Joan Heller Brown for insightful comments. We thank Jean Wang, Erin Foley, Jeffrey Esko, Eva Lee, and Katheryn Meek for helpful reagents. We acknowledge the following funding support: NIH T32-DK07541 to S.F.K.; American Cancer Society Postdoctoral Awards PF-11-027-01-CSM, PF-13-367-01-CDD, and 115095-PF-08-228-01-CSM to H.C.D., M.D.B., and M.M.N., respectively; Era of Hope Scholar Award W81XWH-10-1-0822 to S.J.F.; NIH Director's New Innovator Award DP2-OD004265 to S.J.F.; and a Burroughs Wellcome Fund Career Award in the Biomedical Sciences to S.J.F.

REFERENCES

Anderson CW. DNA damage and the DNA-activated protein kinase. Trends Biochem. Sci. 1993; 18:433–437. [PubMed: 8291090]

Azzoli CG, Temin S, Aliff T, Baker S Jr. Brahmer J, Johnson DH, Laskin JL, Masters G, Milton D, Nordquist L, et al. American Society of Clinical Oncology. 2011 Focused Update of 2009 American Society of Clinical Oncology Clinical Practice Guideline Update on Chemotherapy for Stage IV Non-Small-Cell Lung Cancer. J. Clin. Oncol. 2011; 29:3825–3831. [PubMed: 21900105]

Bell AW, Ward MA, Blackstock WP, Freeman HN, Choudhary JS, Lewis AP, Chotai D, Fazel A, Gushue JN, Paiement J, et al. Proteomics characterization of abundant Golgi membrane proteins. J. Biol. Chem. 2001; 276:5152–5165. [PubMed: 11042173]

Bishé B, Syed GH, Field SJ, Siddiqui A. Role of phosphatidylinositol 4-phosphate (PI4P) and its binding protein GOLPH3 in hepatitis C virus secretion. J. Biol. Chem. 2012; 287:27637–27647. [PubMed: 22745132]

Blunt T, Finnie NJ, Taccioli GE, Smith GC, Demengeot J, Gottlieb TM, Mizuta R, Varghese AJ, Alt FW, Jeggo PA, Jackson SP. Defective DNA-dependent protein kinase activity is linked to V(D)J recombination and DNA repair defects associated with the murine scid mutation. Cell. 1995; 80:813–823. [PubMed: 7889575]

Carpenter AE, Jones TR, Lamprecht MR, Clarke C, Kang IH, Friman O, Guertin DA, Chang JH, Lindquist RA, Moffat J, et al. CellProfiler: image analysis software for identifying and quantifying cell pheno-types. Genome Biol. 2006; 7:R100. [PubMed: 17076895]

Charrier J-D, Durrant SJ, Golec JMC, Kay DP, Knegtel RMA, MacCormick S, Mortimore M, O'Donnell ME, Pinder JL, Reaper PM, et al. Discovery of potent and selective inhibitors of ataxia telangiectasia mutated and Rad3 related (ATR) protein kinase as potential anticancer agents. J. Med. Chem. 2011; 54:2320–2330. [PubMed: 21413798]

Chiu R, Novikov L, Mukherjee S, Shields D. A caspase cleavage fragment of p115 induces fragmentation of the Golgi apparatus and apoptosis. J. Cell Biol. 2002; 159:637–648. [PubMed: 12438416]

Ciccia A, Elledge SJ. The DNA damage response: making it safe to play with knives. Mol. Cell. 2010; 40:179–204. [PubMed: 20965415]

Dippold HC, Ng MM, Farber-Katz SE, Lee S-K, Kerr ML, Peterman MC, Sim R, Wiharto PA, Galbraith KA, Madhavarapu S, et al. GOLPH3 bridges phosphatidylinositol-4- phosphate and actomyosin to stretch and shape the Golgi to promote budding. Cell. 2009; 139:337–351. [PubMed: 19837035]

Godi A, Di Campli A, Konstantakopoulos A, Di Tullio G, Alessi DR, Kular GS, Daniele T, Marra P, Lucocq JM, De Matteis MA. FAPPs control Golgi-to-cell-surface membrane traffic by binding to ARF and PtdIns(4). P. Nat. Cell Biol. 2004; 6:393–404.

Hammond AT, Glick BS. Dynamics of transitional endoplasmic reticulum sites in vertebrate cells. Mol. Biol. Cell. 2000; 11:3013–3030. [PubMed: 10982397]

Hennequin C, Giocanti N, Balosso J, Favaudon V. Interaction of ionizing radiation with the topoisomerase I poison camptothecin in growing V-79 and HeLa cells. Cancer Res. 1994; 54:1720–1728. [PubMed: 8137287]

Hickson I, Zhao Y, Richardson CJ, Green SJ, Martin NMB, Orr AI, Reaper PM, Jackson SP, Curtin NJ, Smith GCM. Identification and characterization of a novel and specific inhibitor of the ataxia-telangiectasia mutated kinase ATM. Cancer Res. 2004; 64:9152–9159. [PubMed: 15604286]

Hsiang YH, Lihou MG, Liu LF. Arrest of replication forks by drug-stabilized topoisomerase I-DNA cleavable complexes as a mechanism of cell killing by camptothecin. Cancer Res. 1989; 49:5077–5082. [PubMed: 2548710]

Hu B-S, Hu H, Zhu C-Y, Gu Y-L, Li J-P. Overexpression of GOLPH3 is associated with poor clinical outcome in gastric cancer. Tumour Biol. 2013; 34:515–520. [PubMed: 23132295]

Hua X, Yu L, Pan W, Huang X, Liao Z, Xian Q, Fang L, Shen H. Increased expression of Golgi phosphoprotein-3 is associated with tumor aggressiveness and poor prognosis of prostate cancer. Diagn. Pathol. 2012; 7:127. [PubMed: 23006319]

Johnson SA, Hunter T. Kinomics: methods for deciphering the kinome. Nat. Methods. 2005; 2:17–25. [PubMed: 15789031]

Jung EJ, Liu G, Zhou W, Chen X. Myosin VI is a mediator of the p53-dependent cell survival pathway. Mol. Cell. Biol. 2006; 26:2175–2186. [PubMed: 16507995]

Kim ST, Lim DS, Canman CE, Kastan MB. Substrate specificities and identification of putative substrates of ATM kinase family members. J. Biol. Chem. 1999; 274:37538–37543. [PubMed: 10608806]

Kunigou O, Nagao H, Kawabata N, Ishidou Y, Nagano S, Maeda S, Komiya S, Setoguchi T. Role of GOLPH3 and GOLPH3L in the proliferation of human rhabdomyosarcoma. Oncol. Rep. 2011; 26:1337–1342. [PubMed: 21822541]

Lane JD, Lucocq J, Pryde J, Barr FA, Woodman PG, Allan VJ, Lowe M. Caspase-mediated cleavage of the stacking protein GRASP65 is required for Golgi fragmentation during apoptosis. J. Cell Biol. 2002; 156:495–509. [PubMed: 11815631]

Laplante M, Sabatini DM. mTOR signaling at a glance. J. Cell Sci. 2009; 122:3589–3594. [PubMed: 19812304]

Lázaro-Diéguez F, Jiménez N, Barth H, Koster AJ, Renau-Piqueras J, Llopis JL, Burger KN, Egea G. Actin filaments are involved in the maintenance of Golgi cisternae morphology and intra-Golgi pH. Cell Motil. Cytoskeleton. 2006; 63:778–791. [PubMed: 16960891]

Li X-Y, Liu W, Chen S-F, Zhang L-Q, Li X-G, Wang L-X. Expression of the Golgi phosphoprotein-3 gene in human gliomas: a pilot study. J. Neurooncol. 2011; 105:159–163. [PubMed: 21499727]

Li H, Guo L, Chen S-W, Zhao X-H, Zhuang S-M, Wang L-P, Song L-B, Song M. GOLPH3 overexpression correlates with tumor progression and poor prognosis in patients with clinically N0 oral tongue cancer. J. Transl. Med. 2012; 10:168. [PubMed: 22905766]

Liu Q, Chang JW, Wang J, Kang SA, Thoreen CC, Markhard A, Hur W, Zhang J, Sim T, Sabatini DM, Gray NS. Discovery of 1-(4-(4-propionylpiperazin-1-yl)-3-(trifluoromethyl)phenyl)-9-(quinolin-3-yl) benzo[h][1,6]naphthyridin-2(1H)-one as a highly potent, selective mammalian target of rapamycin (mTOR) inhibitor for the treatment of cancer. J. Med. Chem. 2010; 53:7146–7155. [PubMed: 20860370]

Lord CJ, Ashworth A. The DNA damage response and cancer therapy. Nature. 2012; 481:287–294. [PubMed: 22258607]

Mancini M, Machamer CE, Roy S, Nicholson DW, Thornberry NA, Casciola-Rosen LA, Rosen A. Caspase-2 is localized at the Golgi complex and cleaves golgin-160 during apoptosis. J. Cell Biol. 2000; 149:603–612. [PubMed: 10791974]

Maney SK, Johnson AM, Sampath Kumar A, Nair V, Santhosh Kumar TR, Kartha CC. Effect of apoptosis-inducing antitumor agents on endocardial endothelial cells. Cardiovasc. Toxicol. 2011; 11:253–262. [PubMed: 21671064]

Mok J, Kim PM, Lam HYK, Piccirillo S, Zhou X, Jeschke GR, Sheridan DL, Parker SA, Desai V, Jwa M, et al. Deciphering protein kinase specificity through large-scale analysis of yeast phosphorylation site motifs. Sci. Signal. 2010; 3:ra12. [PubMed: 20159853]

Morandell, S.; Yaffe, MB. Exploiting synthetic lethal interactions between DNA damage signaling, checkpoint control, and p53 for targeted cancer therapy.. In: Paul, W.; Doetsch, editors. Progress in Molecular Biology and Translational Science. Academic Press; New York: 2012. p. 289-314.

Myers AP, Cantley LC. Targeting a Common Collaborator in Cancer Development. Sci Transl Med. 2010; 2:48ps45–48ps45.

Neal JA, Meek K. Choosing the right path: does DNA-PK help make the decision? Mutat. Res. 2011; 711:73–86. [PubMed: 21376743]

Ng MM, Dippold HC, Buschman MD, Noakes CJ, Field SJ. GOLPH3L antagonizes GOLPH3 to determine Golgi morphology. Mol. Biol. Cell. 2013; 24:796–808. [PubMed: 23345592]

O'Neill T, Dwyer AJ, Ziv Y, Chan DW, Lees-Miller SP, Abraham RH, Lai JH, Hill D, Shiloh Y, Cantley LC, Rathbun GA. Utilization of oriented peptide libraries to identify substrate motifs selected by ATM. J. Biol. Chem. 2000; 275:22719–22727. [PubMed: 10801797]

Obenauer JC, Cantley LC, Yaffe MB. Scansite 2.0: Proteome-wide prediction of cell signaling interactions using short sequence motifs. Nucleic Acids Res. 2003; 31:3635–3641. [PubMed: 12824383]

Peng Y, Zhang Q, Nagasawa H, Okayasu R, Liber HL, Bedford JS. Silencing expression of the catalytic subunit of DNA-dependent protein kinase by small interfering RNA sensitizes human cells for radiation-induced chromosome damage, cell killing, and mutation. Cancer Res. 2002; 62:6400–6404. [PubMed: 12438223]

Presley JF, Cole NB, Schroer TA, Hirschberg K, Zaal KJ, Lippincott-Schwartz J. ER-to-Golgi transport visualized in living cells. Nature. 1997; 389:81–85. [PubMed: 9288971]

Qian H, Yang Y. Alterations of cellular organelles in human liver-derived hepatoma G2 cells induced by adriamycin. Anticancer Drugs. 2009; 20:779–786. [PubMed: 19617817]

Schmitz KR, Liu J, Li S, Setty TG, Wood CS, Burd CG, Ferguson KM. Golgi localization of glycosyltransferases requires a Vps74p oligomer. Dev. Cell. 2008; 14:523–534. [PubMed: 18410729]

Scott KL, Kabbarah O, Liang MC, Ivanova E, Anagnostou V, Wu J, Dhakal S, Wu M, Chen S, Feinberg T, et al. GOLPH3 modulates mTOR signalling and rapamycin sensitivity in cancer. Nature. 2009; 459:1085–1090. [PubMed: 19553991]

Snyder CM, Mardones GA, Ladinsky MS, Howell KE. GMx33 associates with the trans-Golgi matrix in a dynamic manner and sorts within tubules exiting the Golgi. Mol. Biol. Cell. 2006; 17:511–524. [PubMed: 16236792]

Swain SM. Chemotherapy: updates and new perspectives. Oncolo-gist. 2011; 16(Suppl 1):30–39.

Tavecchio M, Munck JM, Cano C, Newell DR, Curtin NJ. Further characterisation of the cellular activity of the DNA-PK inhibitor, NU7441, reveals potential cross-talk with homologous recombination. Cancer Chemother. Pharmacol. 2012; 69:155–164. [PubMed: 21630086]

Thyberg J, Moskalewski S. Role of microtubules in the organization of the Golgi complex. Exp. Cell Res. 1999; 246:263–279. [PubMed: 9925741]

Tu L, Tai WCS, Chen L, Banfield DK. Signal-mediated dynamic retention of glycosyltransferases in the Golgi. Science. 2008; 321:404–407. [PubMed: 18635803]

van Vugt MA, Yaffe MB. Cell cycle re-entry mechanisms after DNA damage checkpoints: giving it some gas to shut off the breaks!. Cell Cycle. 2010; 9:2097–2101. [PubMed: 20505366]

Wang J-H, Chen X-T, Wen Z-S, Zheng M, Deng J-M, Wang M-Z, Lin H-X, Chen K, Li J, Yun J-P, et al. High expression of GOLPH3 in esophageal squamous cell carcinoma correlates with poor prognosis. PLoS ONE. 2012; 7:e45622. [PubMed: 23056210]

Wei J-H, Seemann J. Mitotic division of the mammalian Golgi apparatus. Semin. Cell Dev. Biol. 2009; 20:810–816. [PubMed: 19508856]

Wood CS, Schmitz KR, Bessman NJ, Setty TG, Ferguson KM, Burd CG. PtdIns4P recognition by Vps74/GOLPH3 links PtdIns 4-kinase signaling to retrograde Golgi trafficking. J. Cell Biol. 2009; 187:967–975. [PubMed: 20026658]

Wu CC, Taylor RS, Lane DR, Ladinsky MS, Weisz JA, Howell KE. GMx33: a novel family of trans-Golgi proteins identified by proteomics. Traffic. 2000; 1:963–975. [PubMed: 11208086]

Zeng Z, Lin H, Zhao X, Liu G, Wang X, Xu R, Chen K, Li J, Song L. Overexpression of GOLPH3 promotes proliferation and tumorigenicity in breast cancer via suppression of the FOXO1 transcription factor. Clin. Cancer Res. 2012; 18:4059–4069. [PubMed: 22675169]

Zhou J, Xu T, Qin R, Yan Y, Chen C, Chen Y, Yu H, Xia C, Lu Y, Ding X, et al. Overexpression of Golgi phosphoprotein-3 (GOLPH3) in glioblastoma multiforme is associated with worse prognosis. J. Neurooncol. 2012; 110:195–203. [PubMed: 22972189]

Zhou W, Ryan JJ, Zhou H. Global analyses of sumoylated proteins in Saccharomyces cerevisiae. Induction of protein sumoylation by cellular stresses. J. Biol. Chem. 2004; 279:32262–32268. [PubMed: 15166219]

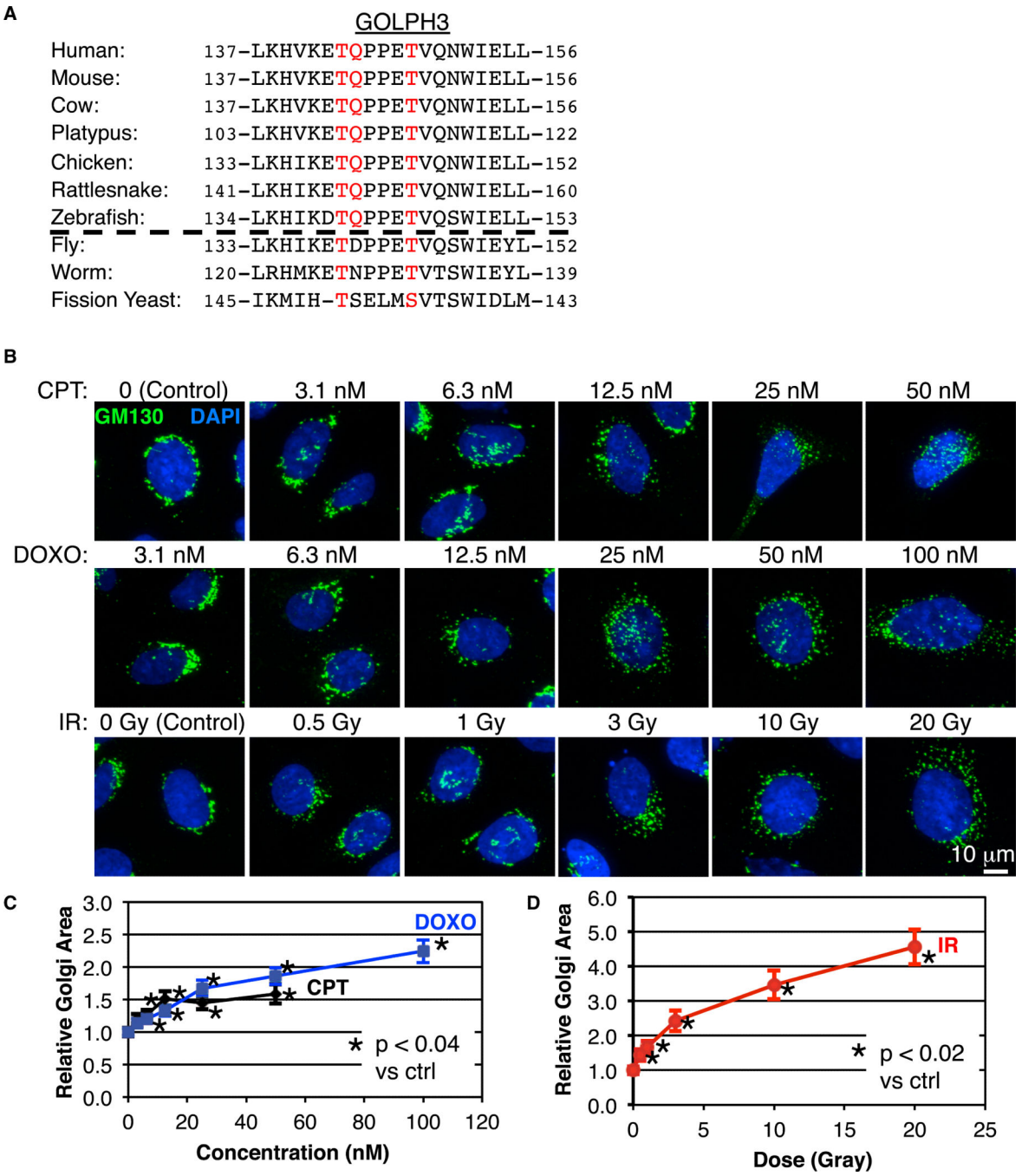

Figure 1. DNA Damage Triggers Golgi Dispersal

(A) Amino acid sequence alignment reveals evolutionary conservation of T143, T148, and the "TQ" motif in GOLPH3. Genomes of organisms listed below the line lack a DNA-PK gene.

(B) Dose response of Golgi to DNA damage. HEK293 cells treated with the indicated doses of CPT or DOXO for 24 hr, or by IR followed by 24 hr of recovery were fixed and stained for GM130 (*cis*-Golgi) and DAPI (DNA).

(C and D) Golgi area per cell was measured relative to control. For each point, n R 21, pooled from three experiments.

In this and all subsequent figures, graphs indicate mean ± SEM, with statistical significance shown (t test). See also Figure S1.

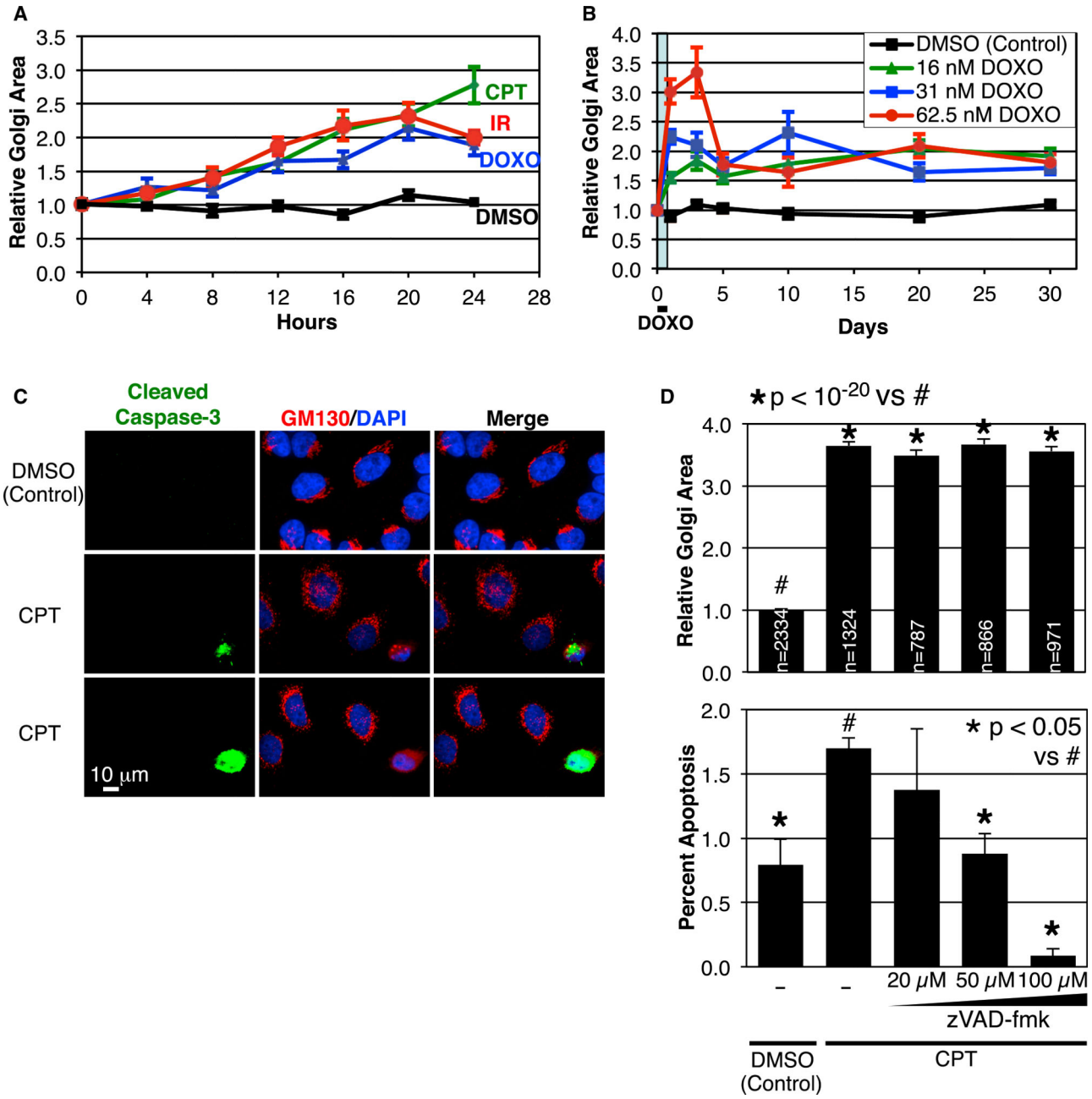

Figure 2. DNA-Damage-Induced Golgi Dispersal Occurs Rapidly, Is Persistent, and Is Independent of Apoptosis

(A) DNA-damage-induced Golgi dispersal in HeLa is detectable within 4 hr and progressively increases over 24 hr. For each treatment, $p < 0.03$ (t test) versus control for all time points after 4 hr; $n < 18$ per point, pooled from three experiments. See also time-lapse imaging in Movies S1 and S2. (B) DNA-damage-induced Golgi dispersal in HeLa is detectable 1 month after treatment with 16–62.5 nM DOXO for 24 hr (shaded). Each concentration of DOXO causes significant Golgi dispersal versus corresponding DMSO-treated cells on each day examined ($p < 0.01$, t test); $n < 29$ per point; pooled from two experiments. (C) HeLa treated with 2 mM CPT or DMSO (control) for 24 hr were stained

with the indicated antibodies and DAPI (DNA). (D) HeLa treated as in (C), but also with zVAD-fmk to inhibit apoptosis. Graphed are the relative Golgi area (top) and number of apoptotic cells (bottom), with the number of cells indicated (n); pooled from three experiments.

See also Figure S2.

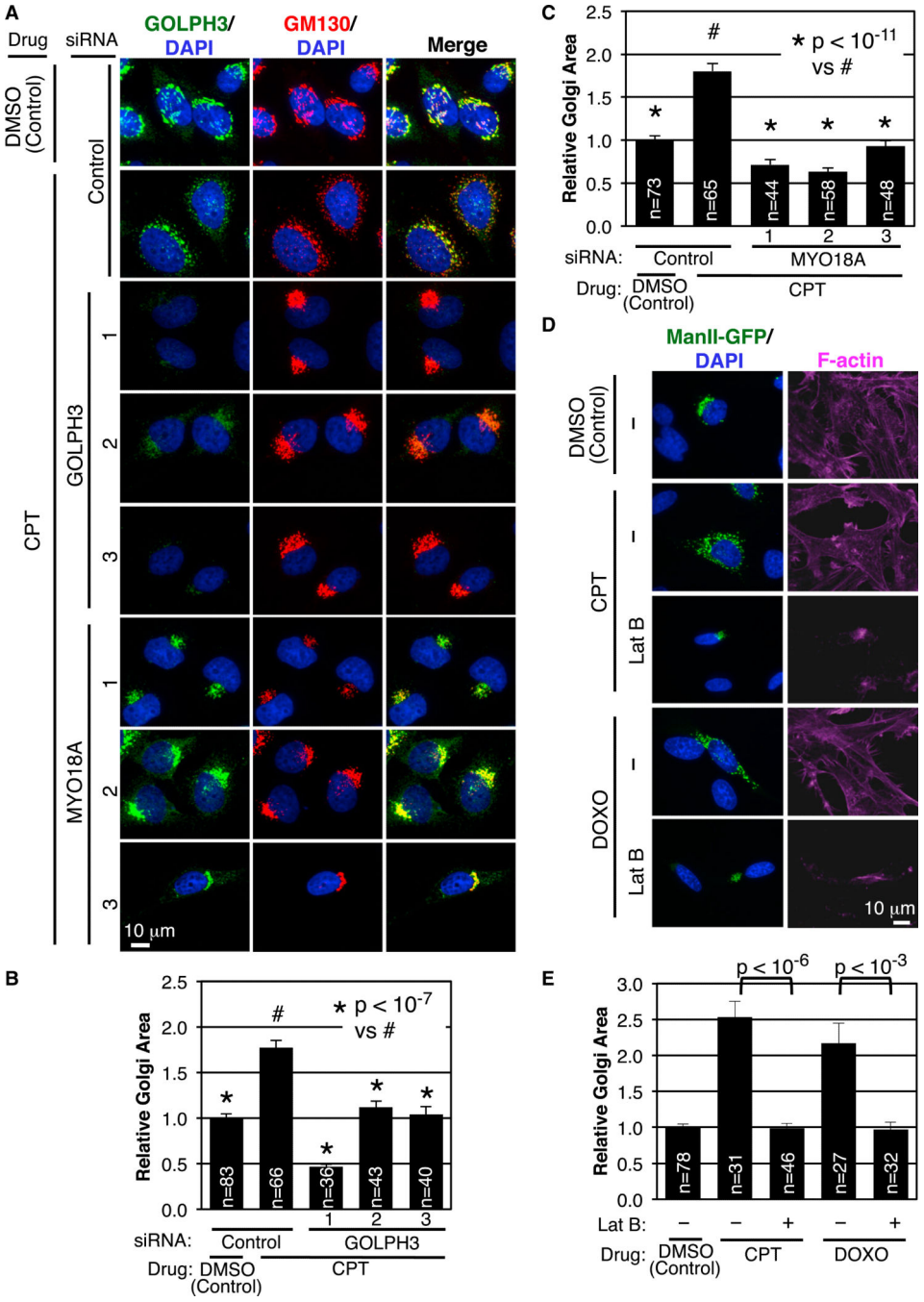

Figure 3. DNA-Damage-Induced Golgi Dispersal Requires GOLPH3, MYO18A, and F-actin

(A) Knockdown in HeLa of GOLPH3 or MYO18A by each of three siRNA oligos (see Figure S3A) prevents CPT (1 μM)-induced Golgi dispersal. Cells were stained with the indicated antibodies and DAPI (DNA).

(B and C) Quantification of Golgi area for (A), with data pooled from two experiments. See Figures S3C and S3E for similar results in HEK293 and HUVECs. (D) Treatment of HeLa with 10 μM Lat B for 10 min reverses Golgi dispersal caused by 1 μM CPT or 1.7 μM DOXO treatment for 17 hr. Golgi is marked by transient expression of ManII-GFP, along

with staining for F-actin (Cy5-phalloidin) and DNA (DAPI). Time-lapse imaging of Lat B treatment is presented in Movie S3. (E) Quantification of Golgi area for (D); pooled from three experiments.

See also Figure S3.

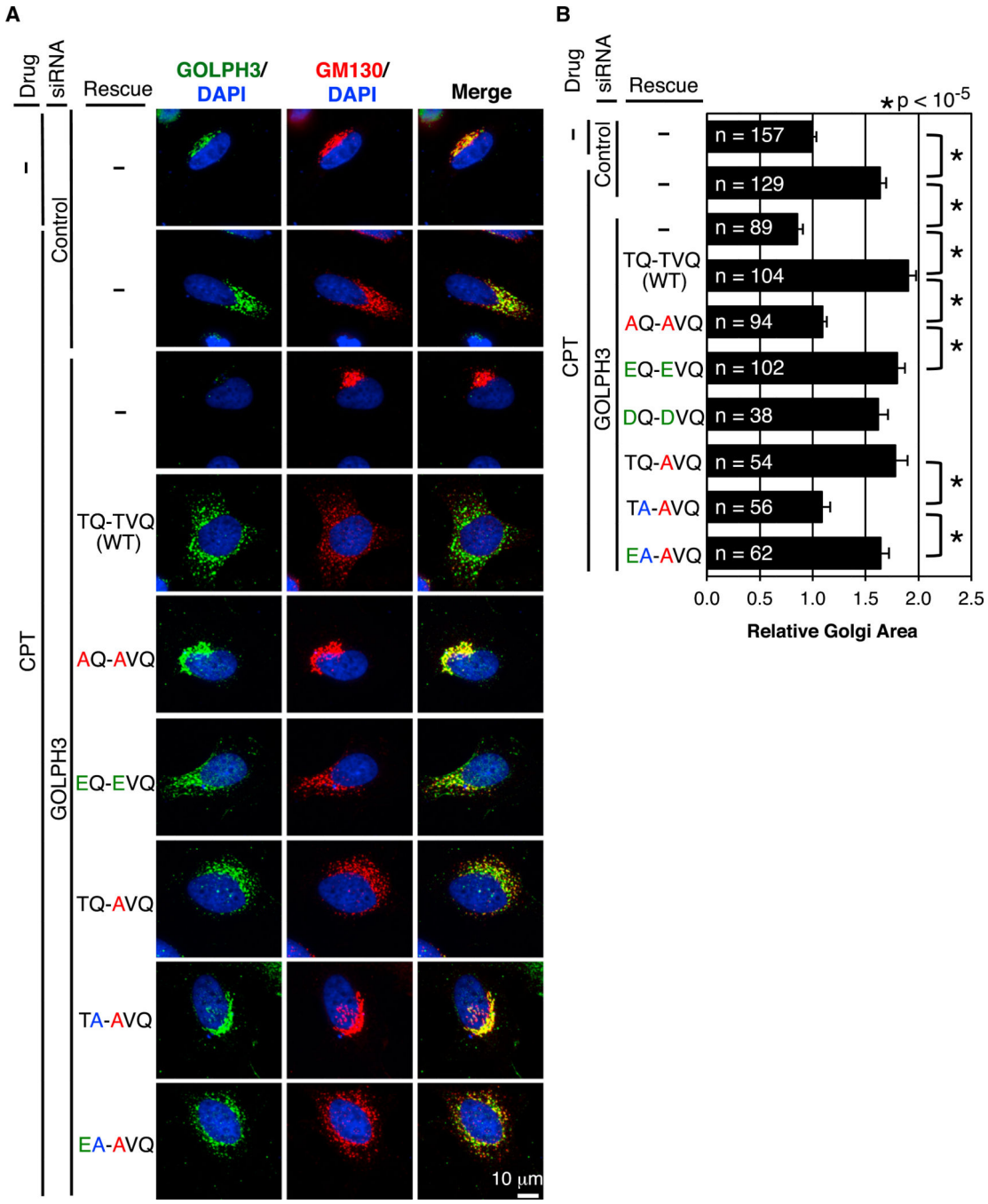

Figure 4. DNA-Damage-Induced Golgi Dispersal Requires the GOLPH3 TQ Motif

(A) HeLa cells were transfected with GOLPH3 or control siRNA and 24 hr later were transiently transfected with the indicated GOLPH3 expression constructs. For the final 24 hr, cells were treated with DMSO (control) or 1 μM CPT. Cells were stained with the indicated antibodies and DAPI (DNA). AQ-AVQ or TA-AVQ mutants rescue the extended Golgi ribbon (see Figures S4A and S4B), but not DNA-damage-induced Golgi dispersal. (B) Quantification of (A), pooled from six (top six) or three (bottom four) experiments. See also Figure S4.

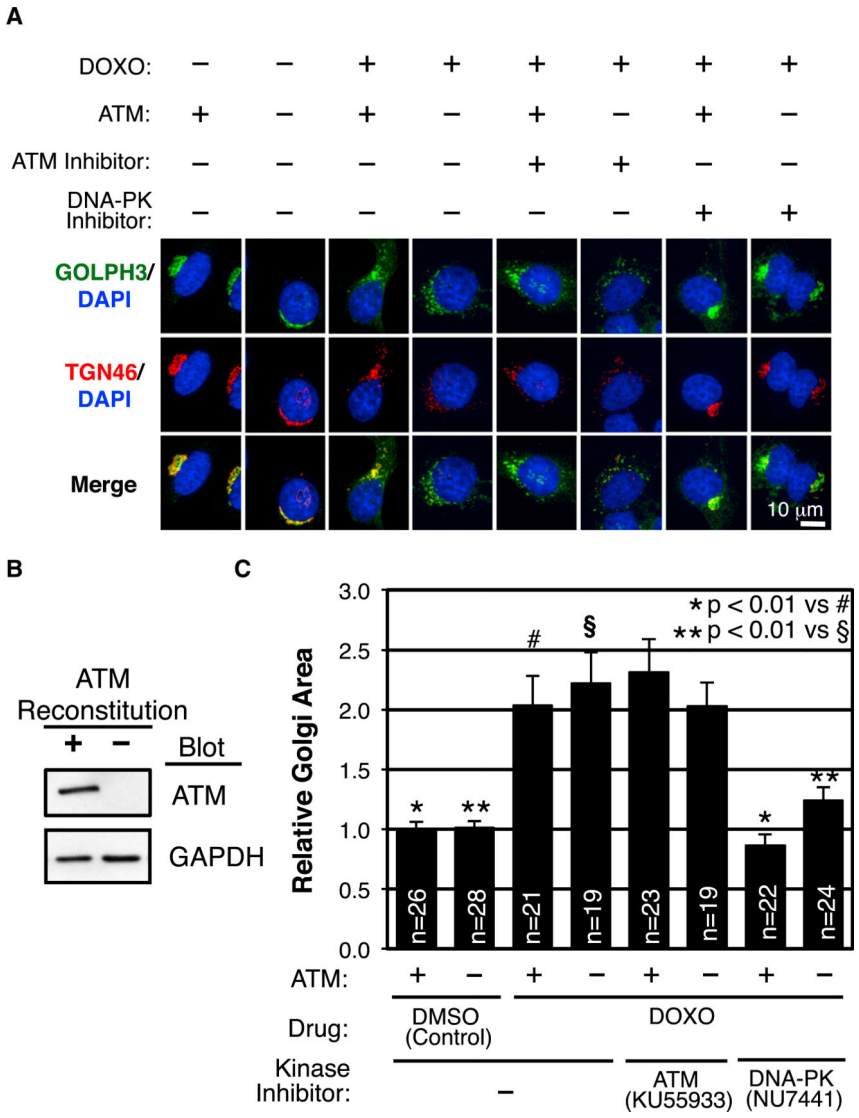

Figure 5. ATM Is Not Required for DNA-Damage-Induced Golgi Dispersal

(A) A-T cells with or without reconstitution of ATM expression were treated for 22.5 hr with 3.4 µM DOXO or DMSO (control) alone or with 10 mM KU55933 or 10 µM NU7441. Cells were stained with the indicated antibodies and DAPI (DNA).

(B) Western blot for ATM shows that A-T cells lack ATM, whereas reconstituted cells express the protein. Blots are representative of three experiments.

(C) Quantification of relative Golgi area for (A). The Golgi disperses regardless of the presence of ATM or treatment with ATM inhibitor. By contrast, DNAPK inhibitor completely prevents DNA-damage-induced Golgi dispersal.

See also Figure S5 and Movie S4.

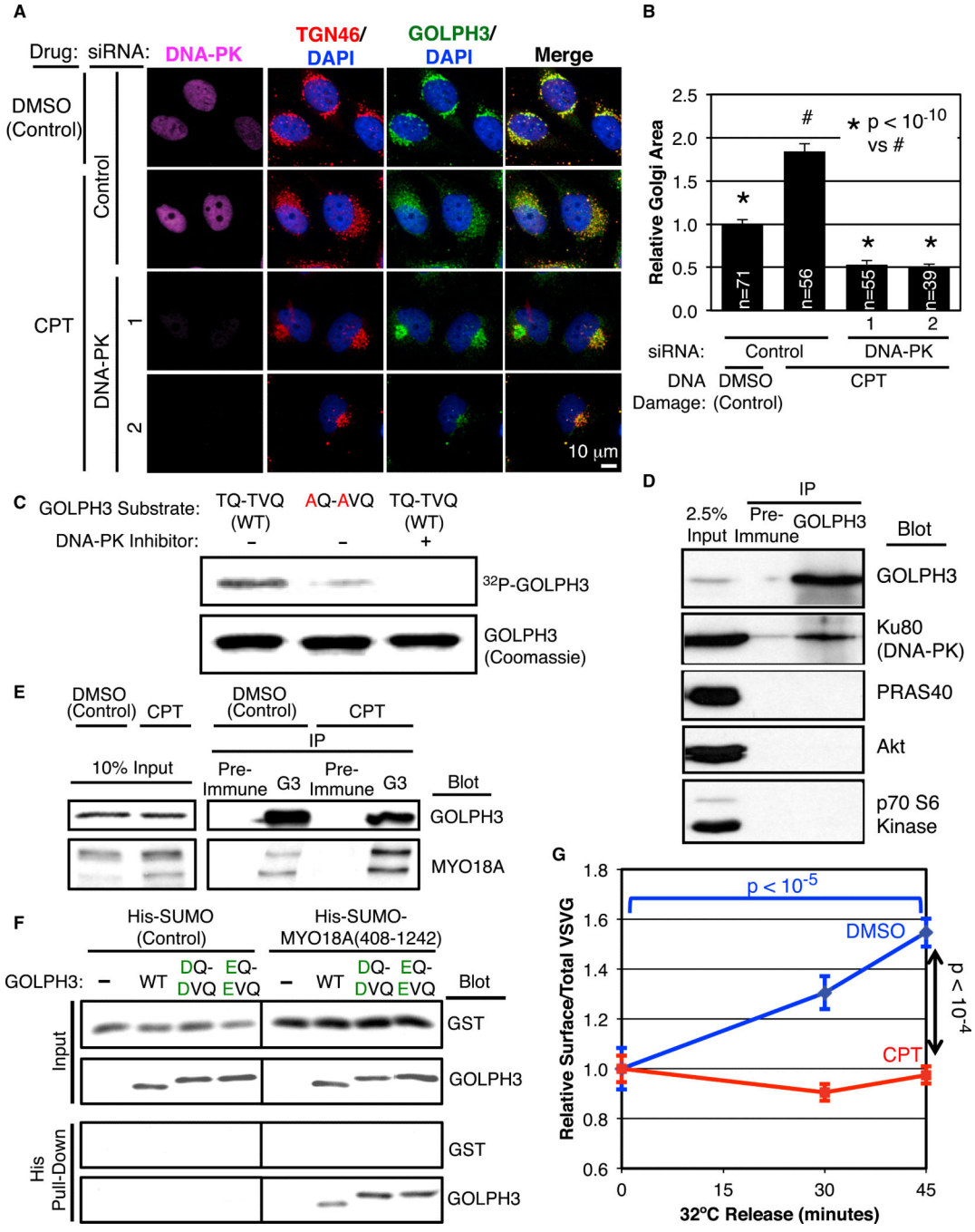

Figure 6. DNA-PK Relays the DNA Damage Signal Directly to GOLPH3 to Trigger Golgi Dispersal

(A) HeLa transfected with the indicated siRNAs and treated with either DMSO (control) or 1 μM CPT for 19 hr were stained with the indicated antibodies and DAPI (DNA).

(B) Quantification of (A). Knockdown of DNA-PK prevents CPT-induced Golgi dispersal. Data pooled from two experiments. See similar results obtained in HEK293 and HUVECs in Figures S3C and S3E.

(C) DNA-PK kinase assay with GST-GOLPH3 TQ-TVQ (WT) or AQ-AVQ mutant, or with addition of 10 mM NU7441. Coomassie stain demonstrates equal loading.

(D) IP of endogenous GOLPH3 from HeLa lysates specifically coimmunoprecipitates the endogenous DNA-PK regulatory subunit Ku80, but not other irrelevant control proteins, as detected by western blot. Results in (C) and (D) are each representative of three experiments.

(E) CoIP/western blotting detects increased interaction between GOLPH3 (G3) and MYO18A after 1 μM CPT for 18 hr versus DMSO control. Input, run on a parallel blot, indicates relative amount of protein in the lysate for each IP. Quantification indicates a 3.7 ± 0.7-fold increase (mean ± SEM) in association of MYO18A with GOLPH3 after CPT; $p < 0.02$ by t test, pooled from six experiments. Similar results for DOXO are shown in Figure S6B.

(F) Pull-down of purified 6xHis-SUMO and 6xHis-SUMO-tagged MYO18A motor domain (aa 408–1,242) with a mixture of purified GST and GOLPH3 (WT or mutant). Compared with WT, DQ-DVQ enhances the GOLPH3/MYO18A interaction by 2.2 ± 0.4-fold, and EQ-EVQ enhances it by 1.9 ± 0.5-fold (mean ± SEM); $p < 0.05$ versus WT (by t test), pooled from five experiments. Vertical line indicates omission of irrelevant intervening lanes. (G) Trafficking of ts045-VSVG-GFP to the PM is significantly impaired in HeLa cells after 1 mM CPT for 18 hr. Quantification of surface VSVG-GFP relative to total VSVG-GFP expression (GFP signal per cell), measured at the nonpermissive temperature (time = 0) or after shift to the permissive temperature (32°C); n = 16–45 per time point, pooled from two experiments. Example images are shown in Figure S6C.

See also Figure S6.

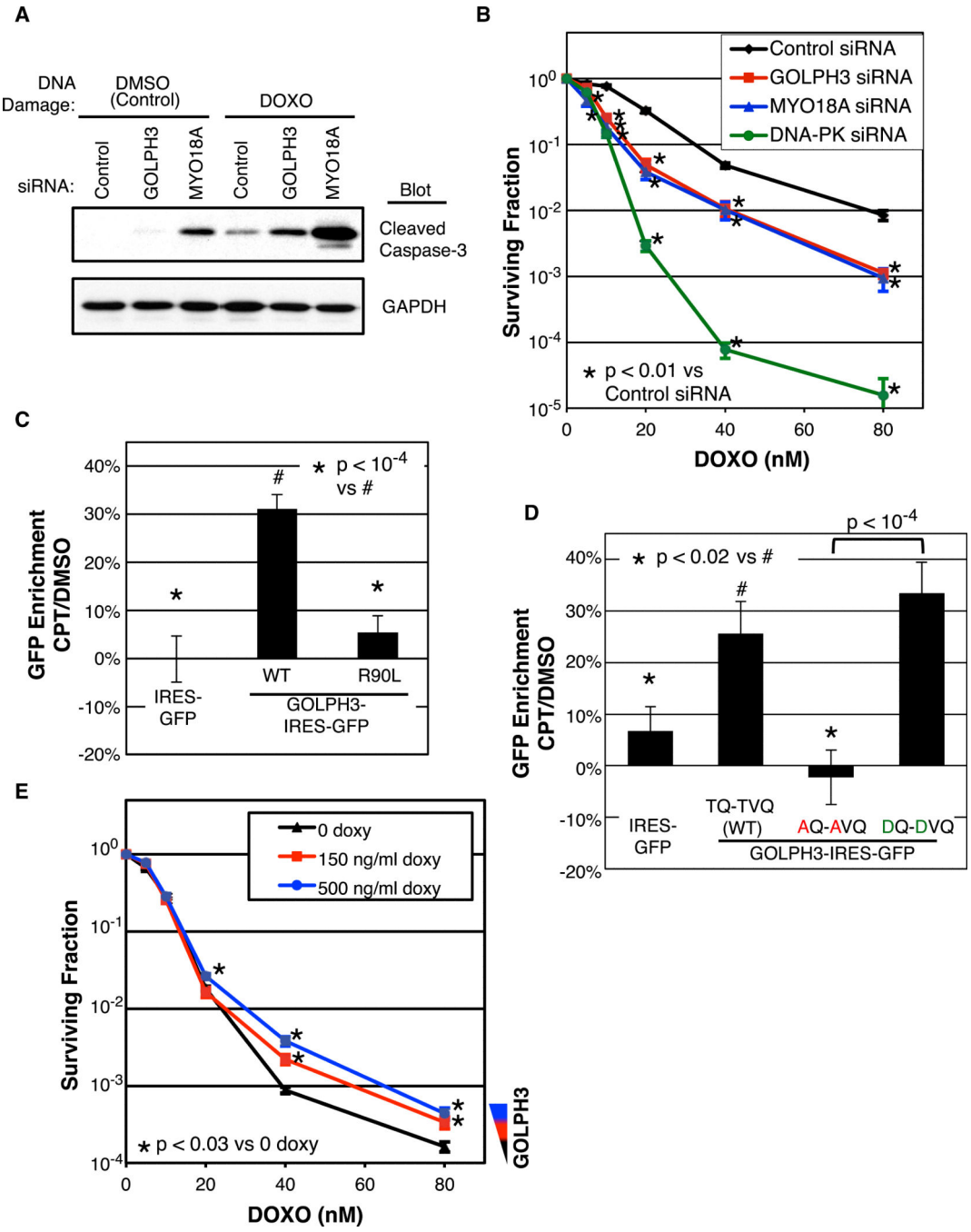

Figure 7. GOLPH3 and MYO18A Modulate Survival after DNA Damage

(A) Knockdown of GOLPH3 or MYO18A increases apoptosis after DNA damage. HeLa cells transfected with the indicated siRNAs after 48 hr were treated with 2 μM DOXO for 24 hr. Cell lysates were blotted for CCasp-3 to detect apoptosis. Results are representative of four experiments.

(B) Clonogenic survival assay of HeLa cells transfected with the indicated siRNAs. Forty-eight hours after siRNA transfection, the cells were replated to produce countable numbers of colonies and then treated with the indicated concentrations of DOXO for 24 hr. Colonies

were counted 10–14 days later. Graphed is the mean ± SEM relative to no treatment. Data are pooled from two (MYO18A siRNA) or three (Control, GOLPH3, and DNA-PK siRNA) experiments, each done in triplicate (n = 6 or 9).

(C) HeLa cell lines were treated with doxycycline to induce overexpression of GFP and GOLPH3, as indicated, in a fraction of cells (western blot shown in Figure S7B), and then treated with 1 μM CPT or DMSO (control) for 24 hr to assess the survival advantage of GFP + cells. Graphed is the increase in the proportion of GFP+ cells that survived after CPT treatment relative to after DMSO treatment. Data are pooled from three experiments, each done in quadruplicate (n = 12).

(D) HeLa survival after DNA damage with transient overexpression of GOLPH3-IRES-GFP or controls, as indicated. Graphed is the increase in the proportion of GFP+ cells that survived after 1 μM CPT treatment relative to after DMSO treatment. Data are pooled from three experiments, each with four to 16 replicates (n = 35 or 36).

(E) Clonogenic survival assay of HeLa cell lines expressing doxycycline-inducible GOLPH3-IRES-GFP. Cells were treated with the indicated concentration of doxycycline (western blot shown in Figure S7C), and then replated and treated with DOXO for 24 hr. Colonies were counted 13 or 14 days later. Data pooled from three (150 ng/ml doxy) to five (0 and 500 ng/ml doxy) experiments, each done in triplicate (n = 9 or 15). Overexpression of GOLPH3 increased cell survival by 4.3-fold, whereas overexpression of IRES-GFP or GOLPH3-R90L-IRES-GFP had no effect on clonogenic survival after DNA damage (Figures S7D and S7E). See also Figure S7.